Down-regulated RPS-30 in *Angiostrongylus cantonensis* L5 plays a defensive role against damage due to oxidative stress

Weiwei Sun
Wenzhou Medical University
Xiumei Yan
Wenzhou Medical University Second Affiliated Hospital
Qing Shi
Wenzhou Medical University
Yuanjiao Zhang
Wenzhou Medical University
Junting Huang
Wenzhou Medical University
Huicong Huang
Wenzhou Medical University
Hongfei Shi
Nanyang Normal University
Baolong Yan (1982ybllog@163.com)
Wenzhou Medical University https://orcid.org/0000-0001-9231-3327

Research

Keywords: Angiostrongylus cantonensis, RPS-30, Caenorhabditis elegans, Oxidative stress, Apoptosis

Posted Date: October 8th, 2020

DOI: https://doi.org/10.21203/rs.3.rs-55501/v2

Version of Record: A version of this preprint was published at Parasites & Vectors on December 9th, 2020.
See the published version at https://doi.org/10.1186/s13071-020-04495-3.

Abstract

Background: Eosinophilic meningitis, caused by *Angiostrongylus cantonensis* L5, is mainly attributed to the Eosinophils, which contribute to tissue inflammatory responses in helminthic infections. Eosinophils are associated with helminthic killing, using the peroxidative oxidation and hydrogen peroxide (H_2O_2) generated by dismutation of superoxide produced during respiratory burst. In contrast, residing in the host with high level of eosinophils, helminthic worms have evolved to attenuate eosinophil-mediated tissue inflammatory responses for their survival in hosts. Our previous study demonstrated that the expression of *Acan-rps-30* was significantly down-regulated in *A. cantonensis* L5 worms, which reside in the cerebrospinal fluid with high level of Eosinophils. *Acan*-RPS-30, a homologous protein of human Fau, which plays a pro-apoptotic regulatory role, may function in protecting worms from oxidative stress.

Methods: RACE, genome Walking, bioinformatics were used to isolate and analyse the structural characterisation of *Acan*-RPS-30; qRT-PCR and microinjection was performed to detect the expression patterns of *Acan-rps-30*; feeding RNAi was used to *ced-3* knock-down; microinjection was performed to construct transgenic worms; oxidative stress assay was used to determine the functions of *Acan*-RPS-30.

Results: Our results showed that *Acan*-RPS-30 consisted of 130 amino acids, and was grouped into Clade V with *C. elegans* in phylogenetic analysis. It was expressed ubiquitously in worms and was down-regulated in both L5 and adult *A. cantonensis*. Worms expressing *pCe-rps30::Acan-rps-30::rfp*, with the refractile “button-like” apoptotic corpses, were susceptible to oxidative stress. Apoptosis genes *ced-3* and *ced-4* were both up-regulated in the transgenic worms. And the phenotype susceptible to oxidative stress could be converted with *ced-3* defective mutation and RNAi. *rps-30*$^{-/-}$ mutant worms were resistant to oxidative stress, with *ced-3* and *ced-4* were both down-regulated. And the oxidative stress resistance phenotype could be rescued and inhibited by expressing *pCe-rps30::Acan-rps-30::rfp* in *rps-30*$^{-/-}$ mutant worms.

Conclusion: In *C. elegans* worms, down-regulated RPS-30 plays a defensive role against damage due to oxidative stress for worm survival by regulating *ced-3* down-regulated. And this might indicate the mechanism of *A. cantonensis* L5 worms, with *Acan*-RPS-30 down-regulated, surviving in the central nervous system of human from immune attack of Eosinophil.

Background

Angiostrongylus cantonensis is a human zoonotic pathogen that may cause eosinophilic meningitis [1]. Several different hosts are required to complete the life cycle of *A. cantonensis*. Human, as an abnormal host, can mainly be infected by accidental ingestion of undercooked intermediate hosts, such as *Pomacea canaliculata*, in which the infective third-stage larvae (iL3) resides [2]. After passage to the small intestine, iL3 will penetrate the blood-brain barrier, and then infects the central nervous system, where it will develop into the fifth-stage larvae (L5), and causes angiostrongyliasis with neurological symptoms [3-6].

Eosinophils, recruited from the circulation into the central nervous system [3], are robust producers of extracellular superoxide due to expression of high level of the enzyme complex that generates superoxide [7], contributing to tissue inflammatory responses and host defense in helminthic infections [8]. Eosinophil peroxidase (EPO), contained in the granule matrix of eosinophils, would be released [9, 10]. EPO is associated with helminthic killing, using the peroxidative oxidation and hydrogen peroxide (H_2O_2) generated by dismutation of superoxide produced during respiratory burst [11-13]. In contrast, residing in the host with high level of eosinophils, helminthic worms have evolved to attenuate eosinophil-mediated tissue inflammatory responses for their survival in hosts [8]. Therefore, *A. cantonensis* L5, residing in the cerebrospinal fluid together with eosinophils, may be resistance to the damage due to oxidative stress. In our previous study, proteomic analysis of different developmental stages using two-dimensional difference gel electrophoresis (2D-DIGE) showed that the expression level of *A. cantonensis* RPS-30 (*Acan*-RPS-30) was lower in L5 than in iL3 [4].

Acan-rps-30 is a homologous gene of human *fau* [14] (FBR-MuSV associated ubiquitously expressed gene), which was originally isolated from a radiation-induced osteosarcoma [15]. *Fau* is inversely inserted as the fox sequence in FBR-MuSV [16, 17], and expression of fox enhances the transformation of FBR-MuSV, presumably by inactivating *fau* expression [18, 19]. *Fau* may play important role in inhibiting tumorigenesis, with down-regulated in both breast cancer [20] and ovarian cancer [21]. Fau is also found to regulate apoptosis in human T-cell lines and HEK293/17 cells [20]. A sequence antisense to *fau* is able to decrease apoptosis induced by dexamethasone, UV or cisplatin in W7.2c cells [19]. In the parasitic nematode *Haemonchus contortus*, RPS-30 can regulate the fourth-stage larval diapauses [22]. *Fau* encodes an ubiquitin-like protein (UBiL), fused to ribosomal protein S30 (S30) as a carboxy-terminal extension [14]. These two products are thought to result from post-translational cleavage [23]. Human Fau-UBiL has 37% amino acid sequence similarity to ubiqutin and contains the C-terminal Gly-Gly dipeptide motif that participates in isopeptide bond formation between ubiquitin and lysine of target proteins [14]. However, a lack of internal lysine residues, sites of poly ubiquitin chain formation, indicates that the biological function of UBiL is different from that of ubiquitin [23]. The identification of UBiL covalently bound to Bcl-G, a member of the Bcl-2 family of apoptosis control proteins [24], suggests a pro-apoptotic regulatory role for *fau*, mediated via Bcl-G [19, 23].

Apoptosis is closely related to oxidative stress in many cell lines, mammalians and the model organism *Caenorhabditis elegans* [25, 26]. Therefore, in this study, we determined the structures and functions of *Acan*-RPS-30 in *A. cantonensis* L5, with the aim of investigating its role in regulating oxidative stress resistance.

Methods

Propagation of *A. cantonensis* and *Caenorhabditis elegans*

A. cantonensis ZJ strain was maintained and propagated in Wenzhou Medical University, China by cycling through the *Pomacea canaliculata* and Sprague-Dawley (SD) rats as described previously [4].

Intermediate hosts *Pomacea canaliculata* were infected with *A. cantonensis* L1 through feeding on rat feces. L3 were collected at 20 days p.i. Infected snails were shelled and crushed. The intestines and other organs were removed and the remaining tissue was homogenized. The homogenates were filtered through a 40-meshsieve, deposited for 5 min at 4 °C, and precipitated 2–3 times at room temperature. The sediments were removed and L3 number and viability were determined by direct observation under a light microscope. Three-week-old Sprague-Dawley (SD) rats (weight 100–120 g, grade clean, Certificate SYXK [ZHE] 2005-0061), supplied by the Laboratory Animal Center of Wenzhou Medical University were orally infected with 50 L3/rat. The rats were housed in polypropylene cages with free access to food and water, and then sacrificed by anesthesia at 25 days and 45 days p.i., respectively. The L3 worms were collected from the intermediate hosts *Pomacea canaliculata*; the L5 harvested from the brains of mice (C57BL/6J (B6), Certificate SYXK (zhe2015-0009)) (non-permissive host same as humans), which were orally infected with 30 L3/mouse; the adult worms were collected from the blood vessels of the hearts and lungs. Individuals of different sexes were separated using morphological criteria: Females are usually longer and thinner than males, and males exhibit typical copulatory bursa. L3, L5, and adults were washed three times with 0.01 mol/L PBS buffer, and stored at −80 °C. These rats were not used for any other part of the study.

Caenorhabditis elegans strains N2, *rps-30* (*tm6034/nt1*) and *ced-3* (*ok2734*) were maintained on Nematode Growth Media (NGM) agar plates at 15 °C as described previously [27]. Worms were fed *Escherichia coli* strain OP50 unless otherwise stated. The mutant strain *ced-3* (*ok2734*) was obtained from the Caenorhabditis Genetic Center (CGC) (University of Minnesota,USA). The mutant strain *rps-30* (*tm6034/nt1*) was originally provided by Shohei Mitani, M.D., Ph.D., Department of Physiology, Tokyo Women's Medical University School of Medicine, Japan. The gene *rsp-30* is essential for survival of the worms, and if the gene is deleted, worms would be sterile. Therefore, the mutant strain *tm6034/nt1* was conducted as trans-heterozygous animals using a balancer nT1, which has fluorescent marker. So, fluorescence positive animals carry nT1 but animals without nT1 are mutation homozygous.

Isolation, purification, treatment and storage of nucleic acids

Total genomic DNA was extracted from *A. cantonensis* ZJ strain adult worms using a small-scale genomic DNA extraction kit (Takara Biotechnology Co., Ltd, Japan). Total RNA was extracted from worms at different developmental stages employing Trizol reagent (Invitrogen, USA), followed by treatment with 2 U of DNase I (Takara Biotechnology Co., Ltd, Japan). First strand cDNA was obtained using the M-MLV RTase cDNA Synthesis Kit (Takara Biotechnology Co., Ltd, Japan). Both DNA and RNA samples were stored at −80 °C.

Isolation of full-length cDNA and genomic DNA encoding *Acan-rps-30* from *A. cantonensis*

Using two degenerate primers, rps-30DF and rps-30DR (Table S1), designed based on a relatively conserved S30 domain, with reference to the *C. elegans* gene (NC_003283.11) and *Homo sapiens* gene (NC_000011.10), a portion of *Acan-rps-30* was amplified by PCR from cDNA synthesized from total RNA extracted from adult worms. PCR products were cloned into the pMD18-T vector (Takara Biotechnology

Co., Ltd, Japan) and sequenced. Based on the available sequence, gene-specific primer pairs (Table S1) were designed. Then, using 5'- and 3'- rapid amplification of cDNA ends (RACE) (Takara Biotechnology Co., Ltd, Japan), two partially overlapping cDNA fragments were obtained. Products were cloned into the pMD18-T vector and sequenced. Based on these sequences, additional primers (Table S1) were designed to amplify full-length *Acan-rps-30*.

Full-length genomic DNA of *Acan-rps-30* from the ZJ strain of *A. cantonensis* was obtained by a Genome Walking kit (Takara Biotechnology Co., Ltd, Japan), using primers designed based on the acquired cDNA sequence (Table S1), following the manufacturer's instructions. The third-round PCR products were cloned into a pMD18-T vector and sequenced.

Bioinformatics analysis

A sequence alignment between *Acan*-RPS-30, *Hs*-RPS-30 (NP_001988.1) and *Ce*-RPS-30 (NP_505007.1) was generated using Clustal Omega. Homology models were built by SWISS-MODEL using *H. sapiens* ribosome (PDB codes 5LKS and 2L7R) as templates. Three-dimensional structural analysis was performed using the PyMOL program. All calculations were carried out under default conditions.

The amino acid sequence inferred for *Acan*-RPS-30 and 7 selected other homologues sequences were subjected to phylogenetic analyses. The phylogenetic analysis was conducted using the neighbour-joining (NJ) and maximum parsimony (MP) methods, respectively, based on the Jones-Taylor-Thornton (JTT) model [28]. Confidence limits were assessed using a bootstrap procedure with 1000 pseudo-replicates for NJ and MP trees, and other settings were obtained using the default values in MEGA v.5.0. A 50% cut-off value was implemented for the consensus tree.

Quantitative real-time PCR (qRT-PCR) analysis

qRT-PCR was performed to determine the abundance of *Acan-rps-30* transcripts in different developmental stages (L3, L5 female,L5 male, Adult female, Adult male) of *A. cantonensis*.

Gene expression levels were determined by RT-PCR using SYBR®Green PCR Master Mix and a 7500 Real-Time PCR System (Applied Biosystems, USA). Relative gene expression was compared with18S ribosomal RNA gene (GenBank: AY295804) as an internal loading control. The target genes and the primers used are listed in Table S1. Statistical analysis was conducted using a one-way ANOVA; $P < 0.05$ was set as the criterion for significance.

RNAi feeding experiments

To generate *ced-3* specific RNAi vectors, *ced-3* cDNAs was cloned into the *L4440* vector. Plasmids were transformed into *E. coli* strain HT115. Primers used for PCR analysis are listed in Table S1. RNAi plates and media were prepared according to [29]. Gravid adults of *C. elegans* were allowed to lay eggs overnight on the RNAi plates and adult worms were picked off. Empty vector-containing *E. coli* were used on separate plates as negative controls.

Transgenic worms

About 2000 bp sequence upstream of *Acan-rps-30* 5'-UTRs was used as putative promoter. To analyze promoter activity of *Acan-rps-30*, the promoter regions of *Acan-rps-30* and *Ce-rps30* were amplified and cloned into plasmid pPD95.77 to construct *pAcan-rps-30::gfp* and *pCe-rps30::gfp*, respectively (Fig. 1A).

To perform cross-species expression of *Acan*-RPS-30 in N2 strain and *rps-30* (*tm6034/nt1*) strains, cDNA sequence was amplified and cloned into pPD95.77 using the promoter of *Ce-rps30* to construct plasmid *pCe-rps-30::Acan-rps-30::rfp* (Fig. 1B). All primers used are listed in Table S1.

Recombinant plasmids were each microinjected into the gonad of young, adult *C. elegans* hermaphrodites as described [2, 30], together with plasmid pRF4 containing a dominant mutant allele of *rol-6* gene, each at a final concentration of 50 µg/mL in the same mixture, using pPD95.77 (*pCe-rps30::gfp*) and pRF4 plasmid mixture as a control. The F2 and subsequent generations with a roller phenotype were analyzed and selected to examine the expression patterns of GFP or RFP, using a fluorescent microscope (Olympus IX71). A minimum of three independent lines expressing each transgene were evaluated.

Fig. 1 Cloning strategy for reporter and rescuing constructs. (A) About 2000 bp sequence upstream of *Acan-rps-30* 5'-UTRs was used as putative promoters. The promoter regions of *Acan-rps-30* and *Ce-rps-30*, fused with green fluorescent protein (GFP) downstream were cloned into plasmid pPD95.77 to construct *pAcan-rps-30::gfp* and *pCe-rps30::gfp*, respectively (B) *Acan-rps-30* cDNA sequence, fused with red fluorescent protein (RFP) downstream was cloned into plasmid pPD95.77, using *pCe-rps30* as promoter, to construct *pCe-rps-30::Acan-rps-30::rfp*.

Oxidative stress assay

The oxidative stress assay was performed as described previously [31]. Briefly, adult hermaphrodites (30 worms/group) were transferred to a 96-well plate containing M9 buffer with 3mM H_2O_2. After incubation at 20°C for the specified durations, the number of dead worms was determined. Worms were scored as dead when they no longer responded with movement to light prodding of the head. Three (H_2O_2) independent experiments were performed. Statistical analysis was performed with Microsoft Excel 2010 software using an unpaired two-tailed *t*-test.

Results

Structural characterisation of Acan-RPS-30

The complete cDNAs of *Acan-rps-30* was isolated by RACE from *A. cantonensis*. *Acan-rps-30* cDNA was 1,209 bp in length, including an open reading frame (ORF) of 393 bp (including stop codon), a 5'-untranslated region (UTR) of 190 bp, and a 3'-UTR of 626 bp (Fig. 2A). 5' UTR harbored the consecutive pyrimidines (TTTCTTTTC), which are commonly found at the 5' end of eukaryotic ribosomal protein

mRNAs [32], and may play a role in regulating translation [33]. The 3' UTR contained the hexamer AATAAA (positions, 612 bp downstream of the TAA). The complete *Acan-rps-30* gene, isolated by Genome Walking from genomic DNA of *A. cantonensis* was 2,967 bp in length, consisting of 4 exons and 3 introns (Fig. 2A).

To characterize the structure of *Acan*-RPS-S30, sequence alignment and structural analysis were performed. The cDNA of *Acan-rps-30* encoded predicted proteins of 130 amino acids (Fig. 2B), which contained the potential cleavage sites (Gly-Gly) of the fusion protein (ubiquitin-like; UBiL-ribosome protein S30; S30). The amino acids sequence was aligned with *Ce*-RPS-30 and *Hs*-RPS-30 (Fig. 2B). The results showed that the C-terminal S30 domains were conserved (*Acan*-RPS-S30 versus *Ce*-RPS-S30 and *Hs*-RPS-30, 87.9% and 77.6% similarity, respectively), whereas the N-terminal UBiL domains were divergent (37.5% and 30.4% similarity, respectively). The S30 domain contained a nuclear location signal (NLS), KQEKKKKKK, with which RPS-30 can go into the nucleus and involves itself in the small subunit assembly of ribosome. Structural analysis from homology models revealed that UBiL region possessed 3 β-sheets and 2 α-helixes (Fig. 2C), and S30 region contained 2 α-helixes (Fig. 2D). The UBiL region did not harbor the K48 and K63 residues, sites of poly ubiquitin chain formation, consisted with the orthologues from other species, indicated the different functions [23], though the structure of UBiL was similar to that of ubiquitin.

Fig. 2 Structure and sequence analysis of *Acan*-RPS-S30. (A) The exon-intron organization of *Acan-rps-30* from *A. cantonensis*. The *Acan-rps-30* gene spans 2,967 bp, consisting of 4 exons and 3 introns. Narrow bar represented untranscribed sequences or introns; wide bars represented exons; brown blocks, coding regions; grey blocks, non-coding 5'- and 3'- untranslated region (UTR). (B) Alignment of amino acid sequences of *Acan*-RPS-S30 from *A. cantonensis* with those from Homo sapiens and *Caenorhabditis elegans*. The accession numbers of sequences available from current databases are: NP_505007.1 (*Ce*-RPS-S30) and NP_001988.1 (*Hs*-RPS-30). Identical and similar residues are shown in black and grey blocks, respectively. The potential cleavage sites (Gly-Gly) of the fusion protein (ubiquitin-like; UBiL-ribosome protein S30; S30) are indicated with green arrows (upstream and downstream sequences are UBiL and S30 regions, respectively). The nuclear location signals in the S30 regions are indicated with a green block. The secondary structural elements of *Acan*-RPS-S30 are shown above the alignment. (C) Predicted tertiary structure of UBiL region, showing 3 β-sheets and 2 α-helixes. (D) Predicted tertiary structure of S30 region, showing 2 α-helixes.

Evolutionary relationship of *Acan*-RPS-30 with RPS-30 orthologues from other nematode species

To determine the evolutionary relationship between *A. cantonensis* and other nematodes, the predicted amino acid sequence of *Acan*-RPS-30 was aligned with orthologs from other nematodes, and subjected to phylogenetic analyses (Fig. 3). *Acan*-RPS-30 clustered closely with *Dv*-RPS-30 from *Dictyocaulus viviparus* with similarity of 89.2%. Cladistic analysis showed that the RPS-30 homologues selected from seven parasitic nematodes were mainly grouped into two clades. *H. contortus*, *Necator americanus*, *D. viviparus* and *A. cantonensis* were in Clade V; *Wuchereria bancrofti*, *Brugia malayi* and *Loa loa* were in

Clade III. This result was in agreement with modern phylogenetic analysis of nematodes [34]. When sequences from the S30 regions only were analysed, bootstrapping did not support the clusters (data not shown). This might indicate that the divergences of the UBiL regions are likely related to species specificity.

Fig. 3 Neighbour-joining phylogenetic tree of RPS-30 proteins from several nematodes. The tree is calculated using the Jones–Taylor–Thornton model in the MEGA program version 5.0. Bootstrap values above the branches (1000 iterations) are shown for robust clades (> 70%). Abbreviation for species names are as follows: Ce: *Caenorhabditis elegans*; Acan: *A. cantonensis*; Dv: *Dictyocaulus viviparous*; Na: *Necator americanus*; Hc: *Haemonchus contortus*; Ll: *Loa loa*; Wb: *Wuchereria bancrofti*; Bm: *Brugia malayi*. The corresponding accession numbers are listed on the right of each species. Clade numbers were noted in Roman numerals.

The expression patterns of *Acan*-rps-30

To determine the relative abundance of *Acan-rps-30* transcript in different developmental stages (L3, L5 and adult) and genders [females (F) and males (M)] of the life cycle of *A. cantonensis*, qRT-PCR was performed with the 18S ribosomal RNA gene as an internal loading control. The results showed that *Acan-rps-30* was transcribed in larval and adult developmental stages examined in different levels (Fig. 4). The expressions of *Acan-rps-30* were significantly down-regulated in both L5 and adult, compared with that in L3; furthermore, the expression level in L5 was greatly lower than that in adult. This might indicate the important roles of *Acan*-RPS-30 in different developmental stages (L3, L5 and adult), which reside in different host.

Fig. 4 Transcriptional profile of *Acan-rps-30* in different developmental stages (L3, L5 and

adult) and genders [females (F) and males (M)] of *A. cantonensis*, determined by real-time PCR analysis. Data shown are mean ± S.E.M derived from three technical replicates with two biological replicates. Relative transcription of the *Acan-rps-30* gene in each sample was calculated by normalisation of the raw data, followed by the determination of abundance relative to the 18S ribosomal RNA gene (GenBank: AY295804), which was served as an internal loading control. Statistical analysis was conducted using a one-way ANOVA. **P* <0.05; ***P*<0.01.

For the lack of functional genetic and in vitro culture methods, it is unable to detect the functions of *Acan*-RPS-30 directly in *A. cantonensis*. Here, *C. elegans*, proposed by numerous authors as a general model for many aspects of basic molecular, cellular and developmental biology in the less tractable parasitic nematodes [34-36], was used to investigate the anatomical expression patterns of *Acan-rps-30* for the closed evolutionary relationship between *A. cantonensis* and *C. elegans*, both belonging to Clade V according to Cladistic analysis [34]. Wild type *C. elegans* (N2 strain) were transformed with the construct *pAcan-rps-30::gfp* and *pCe-rps30::gfp*, respectively (Fig. 1A). Plasmid pRF4 was included in all transformations as a behavioural marker. Transgenic worms showing the roller phenotype were selected. The results showed that GFP under the promoter *pAcan-rps-30* was only expressed in intestine of *C.*

elegans, mainly in the anterior end (Fig. 5A–C), which is the major tissue for lifespan regulation in *C. elegans* [37], in contrast to the situation in worms expressing *pCe-rps-30::gfp*, where GFP was expressed in almost all cells, including intestine, nervous system, pharynx, muscle (Fig. 5D–F). The different activity of *pAcan-rps-30* and *pCe-rps-30* might be due to the heterologous expression, with the low promoter sequences similarity (data not shown). Therefore, *pCe-rps-30* was used as the promoter in following research on the functions of *Acan*-RPS-30 in *C. elegans*.

Fig.5 Expression pattern of *A. cantonensis Acan-rps-30* promoter in *Caenorhabditis elegans*. (A-C) The promoter activity of *Acan-rps-30* in *C. elegans*. *pAcan-rps-30::gfp* is only expressed in intestine, mainly in the anterior end. (D-F) The promoter activity of *Ce-rps-30*. *pCe-rps-30::gfp* is expressed ubiquitously. Arrows indicate the following tissues: i, intestinal; m, muscle; n, neuron; p, pharynx.

Cross-species expressions of *Acan*-RPS-30 in N2 and the *rps-30* deletion mutant worms

In order to clarify the role of *Acan*-RPS-30, cross-species expression of *Acan-rps-30* in *C. elegans* was performed. The expressing constructs containing *Acan-rps-30::rfp* coding sequences driven by *Ce-rps-30* promoters (Fig. 1B), were used to transform *C. elegans* N2 strain and *rps-30* deletion mutant strain *(tm6034)*, respectively. In N2 worms, transformed with *pCe-rps30::Acan-rps-30::rfp*, RFP was expressed widely (Fig. 6B and C), consistent with the *pCe-rps30::gfp* expression pattern(Fig. 5D and F). In addition, RFP mainly focused on the nucleus for the existence of NLS in S30 region. The “button-like” morphology, corpses arising from developmental apoptosis and the gold standard for quantification of apoptosis in *C. elegans* [25], was seen in the anterior pharynx (Fig. 6A and D). This might suggest the pro-apoptotic effect of *Acan*-RPS-30, consistent with the pro-apoptotic regulatory role of *Hs*-RPS-30 [19, 23].

In trans-heterozygous worms *(tm6034)*, the GFP fluorescence positive animals (pharynx), carrying nT1 are heterozygous *rps-30*$^{+/-}$ (Fig. 6E-G), and animals without GFP (nT1) are mutation homozygous *rps-30*$^{-/-}$ (Fig. 6H). After transformation of *pCe-rps30::Acan-rps-30::rfp* in *rps-30*$^{+/-}$ worms, the offspring contained *rps-30*$^{+/-}$ expressing *pCe-rps30::Acan-rps-30::rfp* (Fig. 6I-L) and *rps-30*$^{-/-}$ expressing *pCe-rps30::Acan-rps-30::rfp* (Fig. 6M-P), with the *rps-30*$^{-/-}$ expressing *pCe-rps30::gfp* (Fig. 6Q-S) as the control in the following assay.

Fig.6 Cross-species expressions of *Acan*-RPS-30 in N2 and the *rps-30* deletion mutant worms. (A-D) Expression of *pCe-rps-30::Acan-rps-30::rfp* in N2. RFP was expressed widely; RFP mainly focused on the nucleus; the “button-like” corpses were seen in the anterior pharynx. Arrow heads indicate the corpses. (E-G) The heterozygous *rps-30*$^{+/-}$ worm. The GFP fluorescence positive worms (pharynx) carried the balancer nT1. (H) The homozygous *rps-30*$^{-/-}$ worm. Worms without GFP (nT1) were mutation homozygous *rps-30*$^{-/-}$. (I-L) Expression of *pCe-rps-30::Acan-rps-30::rfp* in the heterozygous *rps-30*$^{+/-}$ worm. RFP was expressed widely, and GFP fluorescence was positive in pharynx. (M-P) Expression of *pCe-rps-30::Acan-rps-30::rfp* in the homozygous *rps-30*$^{-/-}$ worm. RFP was expressed widely, and GFP fluorescence was negative in pharynx. (Q-S) Expression of *pCe-rps-30::gfp* in the homozygous *rps-30*$^{-/-}$ worm.

Functional role of *Acan*-RPS-30 in oxidative stress

To investigate the role of *Acan*-RPS-30 in regulating oxidative stress resistance, we performed oxidative stress assays using H_2O_2. We found that the incidence of rapid death among the N2 worms expressing *pCe-rps30::Acan-rps-30::rfp* was significantly higher than that among the N2 worms expressing *pCe-rps30::gfp*; and the *rps-30* deletion mutants (*rps-30*$^{-/-}$) was significantly more resistant than N2 worms; and this oxidative stress resistance phenotype could be rescued and inhibited by expressing *pCe-rps30::Acan-rps-30::rfp* in *rps-30*$^{-/-}$ mutant worms (Fig. 7A). This might suggest the regulating role of *Acan*-RPS-30 in promoting susceptibility to oxidative stress.

As oxidative stress is considered to be one of the major factors that promote apoptosis [26], we next detect the expression levels of apoptosis genes in *C. elegans*. The results showed that all the apoptosis genes were down-regulated in *rps-30*$^{-/-}$ mutant worms, except *akt-1* up- regulated (Fig. 7B), which inhibits CEP-1 and decreases DNA damage-induced apoptosis [38]; and *ced-3* and *ced-4*, the core apoptosis executive genes [25], were both up-regulated in N2 worms expressing *pCe-rps30::Acan-rps-30::rfp*; Whereas, *ced-9* down-regulated (Fig. 7C), which encodes the homologous protein to the anti-apoptotic B-cell lymphoma 2 (Bcl-2) family of proteins [39].This might indicate the role of *Acan*-RPS-30 in promoting apoptosis in *C. elegans*.

To further determine the effect of apoptosis regulated by *Acan*-RPS-30 on oxidative stress susceptibility, we constructed the *C. elegans* strain *ced-3*$^{-/-}$*(ok2734)* expressing *pCe-rps30::Acan-rps-30::rfp* and the strain N2; *pCe-rps30::Acan-rps-30::rfp* with *ced-3* knocked down using RNA interference. Then, the survival percentages were detected with the strains *ced-3*$^{-/-}$ expressing *pCe-rps30::gfp* and N2; *pCe-rps30::Acan-rps-30::rfp* as controls, respectively. We found that the incidence of rapid death among the worms *ced-3*$^{-/-}$ expressing *pCe-rps30::Acan-rps-30::rfp* was almost the same as that among the worms *ced-3*$^{-/-}$ expressing *pCe-rps30::gfp*; and that among the worms N2 expressing *pCe-rps30::Acan-rps-30::rfp* was significantly higher than that among the worms N2 expressing *pCe-rps30::Acan-rps-30::rfp* with *ced-3* knocked down (Fig. 7D). This might suggest that the regulating role of *Acan*-RPS-30 in promoting susceptibility to oxidative stress was played through CED-3, which is the core executive effector in the worm cell apoptosis [25].

Fig.7 Down-regulated RPS-30 plays a defensive role against oxidative stress by regulating *ced-3*. (A) Oxidative stress assays using H_2O_2 in N2 and *rps-30* mutant worms expressing *pCe-rps30::Acan-rps-30::rfp*. (B) The expression level of apoptosis genes in homozygous *rps-30*$^{-/-}$ worm. (C) The expression level of apoptosis genes in N2 worms expressing *pCe-rps30::Acan-rps-30::rfp*. (D) Oxidative stress assays using H_2O_2 in *ced-3* mutant worms and worms expressing *pCe-rps30::Acan-rps-30::rfp*. The worms were counted as described in the “Methods” section. The error bars indicate standard deviation. **P*<0.05; ***P*<0.01.

Discussion

Eosinophilic meningitis, caused by *A. cantonensis* L5, is mainly attributed to the Eosinophils [40], which contribute to tissue inflammatory responses in helminthic infections [8]. Eosinophils, a well-equipped immune cell recruited from the circulation into inflammatory foci [41] and directly recognizes helminth-derived immunomodulating agents, function in host defense against helminth infection [8]. The cell surface of eosinophils possess a variety of receptors for cell signaling associated with chemotaxis, adhesion, respiratory burst, degranulation, apoptosis or survival [42], all of which may be closely associated with eosinphil-mediated tissue inflammatory responses in helminth infection [8]. Eosinophils mainly contain four main granules: crystalloid granules, primary granules, small granules, and secretory vesicles [43]. Cytotoxic granular proteins, including major basic protein (MBP), eosinophil peroxidase (EPO), eosinophil cationic protein (ECP), and eosinophil-derived neurotoxin (EDN), reside in the crystalloid granules [9, 10]. The functional role of EPO is associated with helminthic killing [44]. EPO catalyzes the peroxidative oxidation of halides and thiocyanate present in the plasma together with hydrogen peroxide (H_2O_2) generated by dismutation of superoxide produced during respiratory burst [11-13]. Eosinophils, the robust producers of extracellular superoxide due to expression of high level of the enzyme complex that generates superoxide [7], produce superoxide anions in response to helminth-derived cysteine proteases [45]. In contrast, residing in the host with high level of eosinophils, helminthic worms have evolved to attenuate eosinophil-mediated tissue inflammatory responses for their survival in hosts, such as inducing apoptosis of eosinophils [46, 47] and blocking the chemotactic effects on eosinophils [48]. Here, we identified *Acan-rps-30* from *A. cantonensis*. The expressions of *Acan-rps-30* were significantly down-regulated in both L5 and adult. Both L5 and adult, residing in mammalian, humans and rats respectively, are attacked by immune response from hosts, such as superoxide produced by eosinophils. Our results showed that *Acan*-RPS-30 could promote susceptibility to hydrogen peroxide, and *rps-30*$^{-/-}$ mutant worms were resistant to oxidative stress. This might indicate the regulating function of *Acan*-RPS-30 in attenuating eosinophil-mediated immue attack upon L5 worms in the central nervous system of human by its lower expression. Whereas, L3 worms, with higher level of *Acan-rps-30*, reside in intermediate hosts (e.g., *Pomacea canaliculata*), in which the immune system are lower than that in mammalians, and the immune attack may be weaker, or even there may be no eosinophil-mediated superoxide attack in snails. Therefore, the higher level of *Acan-rps-30* in L3 worms may indicate its multi-function in different developmental stages, such as promoting the development of L3 worms with S30 region [22]. Furthermore, the expression level in L5 was significantly lower than that in adult, which possesses the thicker cuticle than L5 larva. Though adult worms parasite in the blood vessels of the hearts and lungs of rats, in which there are the senior immune system, with attacked by superoxide from eosinophil, the thick cuticle may provide protection [49], and many other proteins may be differently expressed in the cuticle, such as the homologous gene of *lec-1*, which plays important role against damage due to oxidative stress [4, 49].

A. cantonensis is relatively closely related to the model organism *C. elegans*, both belonging to clade V [2, 34], and the homologous gene of *Acan-rps-30* is *Ce-rps30* (**C26F1.4**). Here, we used *C. elegans* as a surrogate to explore the in vivo functions of the homologous gene, *Acan-rps-30*, for the lack of effective genetic manipulation in parasitic nematode. In *C. elegans*, apoptosis is characterized with the refractile

“button-like” morphology, apoptotic corpses, which are caused by inefficient engulfment from healthy neighboring cells [50-52]. The “button-like” appearance under differential interference contrast (DIC) optics is the gold standard for quantification of apoptosis in *C. elegans* [25]. In this study, the “button-like” corpses were seen in the anterior pharynx of the transgenic worm expressing *pCe-rps30::Acan-rps-30::rfp*, indicating the happening of apoptosis. CED-1 and CED-5 proteins can recognize corpses and are critical to engulfment [50]. The down-regulated expression of *ced-1* and *ced-5* in the transgenic worm expressing *pCe-rps30::Acan-rps-30::rfp* might contribute to the formation of corpses.

Four genes, comprising the core apoptosis pathway in *C. elegans*, have been identified [38, 53]. *egl-1* encodes a proapoptotic BH3-only protein that antagonizes the CED-9 protein [54]. *ced-9*, that functions upstream of *ced-4* to prevent activation of the CED-3 caspase, encodes the homologous protein to the anti-apoptotic B-cell lymphoma 2 (Bcl-2) family of proteins [39]. *ced-3*, encodes a proteolytic caspase protein that is activated by CED-4, the worm homolog of mammalian apoptotic protease activation factor 1 [55]. Therefore, CED-3 is the core executioner [25]. In the worms expressing *pCe-rps30::Acan-rps-30::rfp*, the *ced-3* was up-regulated, and the worms exhibited apoptosis and susceptibility to oxidative stress; whereas, in the *rps-30*$^{-/-}$ mutant worms, the *ced-3* was down-regulated, and the worms exhibited resistance to oxidative stress. This phenotype could be converted with *ced-3* defective mutation and RNAi. Therefore, the function of *Acan*-RPS-30 in promoting susceptibility to oxidative stress might be conducted through apoptosis by regulating CED-3. And in *A. cantonensis* L5, *Acan*-RPS-30 was down-regulated to enhance the resistance to oxidative stress from eosinophils for worms’ survival in host.

Conclusions

This study investigated the structural and functional characterisation of *Acan*-RPS-30 from *A. cantonensis*. We found that *Acan*-RPS-30 could promote worms to be susceptible to oxidative stress through apoptosis by regulating CED-3; and worms, with *Acan*-RPS-30 down-regulated, were resistant to oxidative stress. Our findings may reveal the mechanism for *A. cantonensis* L5 worms surviving in the central nervous system of human from immune attack of Eosinophil.

Declarations

Acknowledgements

We would like to thank Dr. Du A.F. (Institute of Preventive Veterinary Medicine, Zhejiang University, China), for her assistance with transgenic techniques in *C. elegans* and gifts of required vectors. The *C. elegans* strains, N2 and *ced-3* (*ok2734*) were originally provided by the Caenorhabditis Genetics Center,University of Minnesota, which is funded by the NIH National Center for Research Resources. The *C. elegans* strain *rps-30* (*tm6034/nt1*) was originally provided by Shohei Mitani, M.D., Ph.D., Department of Physiology, Tokyo Women's Medical University School of Medicine, Japan.

Authors’ contributions

BLY, HCH and HFS conceived and designed the experiments. WWS, XMY and BLY wrote the manuscript. WWS, XMY, QS and YJZ performed the experiments. JTH and YJZ collected and analyzed the data. HCH, BLY and HFS participated in technological guidance and coordination. All authors read and approved the final manuscript.

Funding

This project was supported by grants from the Natural Science Foundation of Zhejiang Province of China (Nos. LY17H070004 and LQ17H190005) and the National Natural Science Foundation of China (Nos. 81471234 and 31902263). The funders had no role in study design, data collection and analysis, decision to publish, or preparation of the manuscript.

Availability of data and materials

Data supporting the conclusions of this article are included within the article and its additional files. The datasets used in the present study are available from the corresponding author upon reasonable request.

Ethics approval and consent to participate

All the experimental animals used were treated strictly in accordance with the recommendations in the Guide for the Regulation for the Administration of Affairs Concerning Experimental Animal of the People's Republic of China. The protocol employed was approved by Laboratory Animal Ethics Committee of Wenzhou Medical College & Laboratory Animal Centre of Wenzhou Medical College (Permit Numbers: SYXK (zhe2015-0009) and SYXK [ZHE] 2005-0061). The care and maintenance of animals followed this institution's guidelines.

Consent for publication

Not applicable.

Competing interests

The authors declare that they have no conflicts of interests.

References

1. Lv S, Zhang Y, Steinmann P, Utzinger J, Zhou XN. The genetic variation of *Angiostrongylus cantonensis* in the People's Republic of China. Infect Dis Poverty. 2017;6:125–36.
2. Yan BL, Sun WW, Shi XM, Huang LY, Chen LZ, Wang SH, Yan LZ, Liang SH, Huang HC. *Angiostrongylus cantonensis* daf-2 regulates dauer, longevity and stress in *Caenorhabditis elegans*. Vet Parasitol. 2017;240:1–10.

3. Chen KY, Chiu CH, Wang LC. Anti-apoptotic effects of Sonic hedgehog signalling through oxidative stress reduction in astrocytes co-cultured with excretory-secretory products of larval *Angiostrongylus cantonensis*. Sci Rep. 2017;7:41574.
4. Huang HC, Yao LL, Song ZM, Li XP, Hua QQ, Li Q, et al. Development specific differences in the proteomics of *Angiostrongylus cantonensis*. PLoS One. 2013;8:e76982.
5. Yii CY. Clinical observations on eosinophilic meningitis and meningoencephalitis caused by *Angiostrongylus cantonensis* on Taiwan. Am J Trop Med Hyg. 1976;25:233–49.
6. Martins YC, Tanowitz HB, Kazacos KR. Central nervous system manifestations of Angiostrongylus cantonensis infection. Acta Trop. 2015;141:46–53.
7. Someya A, Nishijima K, Nunoi H, Irie S, Nagaoka I. Study on the superoxide-producing enzyme of eosinophils and neutrophils: comparison of the NADPH oxidase components. Arch Biochem Biophys. 1997;345:207–13.
8. Shin MH, Lee YA, Min DY. Eosinophil-Mediated Tissue Inflammatory Responses in Helminth Infection. Korean J Parasitol. 2009;47:125–131.
9. Egesten A, Alumets J, von Mecklenburg C, Palmegren M, Olsson I. Localization of eosinophil cationic protein, major basic protein, and eosinophil peroxidase in human eosinophils by immunoelectron microscopic technique. J Histochem Cytochem. 1986;34:1399–403.
10. Peters MS, Rodriguez M, Gleich GJ. Localization of human eosinophil granule major basic protein, eosinophil cationic protein, and eosinophil-derived neurotoxin by immunoelectron microscopy. Lab Invest. 1986;54:656–62.
11. Weiss SJ, Test ST, Eckmann CM, Roos D, Regiani S. Brominating oxidants generated by human eosinophils. Science. 1986;234:200–3.
12. Mayeno AN, Curran AJ, Roberts RL, Foote CS. Eosinophils preferentially use bromide to generate halogenating agents. J Biol Chem. 1989;264:5660–8.
13. Thomas EL, Bozeman PM, Jefferson MM, & King CC. Oxidation of bromide by the human leukocyte enzymes myeloperoxidase and eosinophil peroxidase. Formation of bromamines. J Biol Chem. 1995;270:2906–13.
14. Kas K, Michiels L, Merregaert J. Genomic structure and expression of the human fau gene: encoding the ribosomal protein 30 fusion to a ubiquitin-like protein. Biochem Biophys Res Commun. 1992;187:927–933.
15. Finkel MP, Reilly Jr CA, Biskis BO. Pathogenesis of radiation and virus induced bone tumors. Recent Results Cancer Res. 1976;54:92–103.
16. Van Beveren C, Enami S, Curran T, Verma IM. FBR murine osteosarcoma virus. II. Nucleotide sequence of the provirus reveals that the genome contains sequences acquired from two cellular genes. Virology. 1984;135:229–243.
17. Olvera J, Wool IG. The carboxyl extension of a ubiquitin-like protein is rat ribosomal protein S30. J Biol Chem. 1993;268:17967–17974.

18. Michiels L, Van der Rauwelaert E, Van Hasselt F, Kas K, Merregaert J. Fau cDNA encodes a ubiquitin-like S30 fusion protein and is expressed as an antisense sequence in FBR murine sarcoma virus. Oncogene. 1993;8:2537–2546.
19. Mourtada-Maarabouni M, Kirkham L, Farzaneh F, Williams GT. Regulation of apoptosis by fau reveal by functional expression cloning and antisense expression. Oncogene. 2004;23:9419–9426.
20. Pickard MR, Green AR, Ellis IO, Caldas C, Hedge VL. Mourtada-Maarabouni M, Williams GT. Dysregulated expression of Fau and MELK is associated with poor prognosis in breast cancer. Breast Cancer Res. 2009;11:R60.
21. Moss EL, Mourtada-Maarabouni M, Pickard MR, Redman CW, Williams GT. FAU regulates carboplatin resistance in ovarian cancer. Gene Chromosome Canc. 2010;49:70–77.
22. Yan, BL, Guo XL, Zhou QJ, Yang Y, Chen XQ, Sun WW, Du AF. *Hc-fau*, a novel gene regulating diapause in the nematode parasite *Haemonchus contortus*. Int J Parasitol. 2014;44:775–786.
23. Pickard MR, Mourtada-Maarabouni M, Williams GT. Candidate tumour suppressor Fau regulates apoptosis in human cells: an essential role for Bcl-G. Biochim Biophys Acta. 2011;1812:1146–1153.
24. Nakamura M, Tanigawa Y. Characterization of ubiquitin-like polypeptide acceptor protein, a novel pro-apoptotic member of the Bcl2 family. Eur J Biochem. 2003;270:4052–4058.
25. Lant B, Brent Derry W. Analysis of Apoptosis in *Caenorhabditis elegans*. Cold Spring Harb Protoc. 2014;doi:10.1101/pdb.top070458.
26. Buttke TM, Sandstrom PA. Oxidative stress as a mediator of apoptosis. Immunol Today. 1994;15:7–10.
27. Brenner S. The genetics of *Caenorhabditis elegans*. Genetics. 1974;77:71–94.
28. Tamura K, Peterson D, Peterson N, Stecher G, Nei M. MEGA5:molecular evolutionary genetics analysis using maximum likelihood, evolutionary distance, and maximum parsimony methods. Mol Biol Evol. 2011;28:2731–2739.
29. Kwon ES, Narasimhan SD, Yen K, Tissenbaum HA. A new DAF-16 isoform regulates longevity. Nature. 2010;466:498–502.
30. Mello CC, Kramer JM, Stinchcomb D, Ambros V. Efficient gene transfer in *elegans*: extrachromosomal maintenance and integration of transforming sequences. EMBO J. 1991;10:3959–3970.
31. Nemoto-Sasaki Y, Kasai K. Deletion of *lec-10*, a galectin-encoding gene, increases susceptibility to oxidative stress in *Caenorhabditis elegans*. Biol Pharm Bull. 2009;32:1973–1977.
32. Olvera J, Wool IG. The carboxyl extension of a ubiquitin-like protein is rat ribosomal protein S30. J Biol Chem. 1993;268:17967–17974.
33. Levy S, Avni D, Hariharan N, Perry RP, Meyuhas O. Oligopyrimidine tract at the 50 end of mammalian ribosomal protein mRNAs is required for their translational control. Proc Natl Acad Sci. U.S.A. 1991;88:3319–3323.
34. Blaxter M. *Caenorhabditis elegans* is a nematode. Science. 1998;282:2041–2046.

35. Bürglin TR, Lobos E, Blaxter ML. *Caenorhabditis elegans* as a model forparasitic nematodes. Int J Parasitol. 1998;28:395–411.
36. Aboobaker AA, Blaxter ML. Medical significance of *Caenorhabditis elegans.* Ann Med. 2000;32:23–30.
37. Libina N, Berman JR, Kenyon C. Tissue-specific activities of *elegans* DAF-16 in the regulation of lifespan. Cell. 2003;115:489–502.
38. Gartner A, Milstein S, Ahmed S, Hodgkin J, Hengartner MO. A conserved checkpoint pathway mediates DNA damage-induced apoptosis and cell cycle arrest in *elegans*. Mol Cell. 2000;5:435–443.
39. Hengartner MO, Horvitz HR. Activation of *elegans* cell death protein CED-9 by an amino-acid substitution in a domain conserved in Bcl-2. Nature. 1994;369:318–320.
40. David GP, Christian MM, Alberto Juan DC. Human neuroimmune response against *Angiostrongylus cantonensis*. Revista Cubana de Investigaciones Biomédicas. 2019;38:e100.
41. Rosenberg HF, Phipps S, Foster PS. Eosinophil trafficking in allergy and asthma. J Allergy Clin Immunol. 2007;119:1303-1310.
42. Hogan SP, Rosenberg HF, Moqbel R, Phipps S, Foster PS, Lacy P, Kay AB, Rothenberg ME. Eosinophils: Biological properties and role in health and disease. Clin Exp Allergy. 2008;38:709-750.
43. Dvorak AM, Weller PF. Ultrastructural analysis of human eosinphils. Chem Immunol. 2000;76:1-28.
44. Hogan SP, Rosenberg HF, Moqbel R, Phipps M, Foster PS, Lacy P, Barry Kay A, Rothenberg ME. Eosinophils: Biological Properties and Role in Health and Disease. Clinical and Experimental Allergy. 2008;38:709–750.
45. Chung YB, Kita H, Shin MH. A 27 kDa cysteine protease secreted by newly excysted Paragonimus westermani metacercariae induces superoxide anion production and degranulation of human eosinophils. Korean J Parasitol. 2008;46:95–99.
46. Min DY, Lee YA, Ryu JS, Ahn MH, Chung YB, Sim S, Shin MH. Caspase-3-mediated apoptosis of human eosinophils by the tissue-invading helminth Paragonimus westermani. Int Arch Allergy Immunol. 2004;133:357–364.
47. Serradell MC, Guasconi L, Cervi L, Chiapello LS, Masih DT. Excretory-secretory products from Fasciola hepatica induce eosinophil apoptosis by a caspase-dependent mechanism. Vet Immunol Immunopathol. 2007;117:197–208.
48. Culley FJ, Brown A, Conroy DM, Sabroe I, Pritchard DI, Williams TJ. Eotaxin is specifically cleaved by hookworm metalloproteases preventing its action in vitro and in vivo. J Immunol. 2000;165:6447–6453.
49. Tomoharu T, Yoko NS, Sugiura K, Arata Y, Kasai K. Galectin LEC-1 plays a defensive role against damage due to oxidative stress in *Caenorhabditis elegans*. J Biol Chem. 2013;154(5):455–464.
50. Ellis RE, Jacobson DM, Horvitz HR. Genes required for the engulfment of cell corpses during programmed cell death in *Caenorhabditis elegans*. Genetics. 1991;129:79–94.

51. Grimsley C, Ravichandran KS. Cues for apoptotic cell engulfment: Eat-me, don't eat-me and come-get-me signals. Trends Cell Biol. 2003;13:648–656.
52. Kinchen JM, Ravichandran KS. Journey to the grave: Signaling events regulating removal of apoptotic cells. J Cell Sci. 2007;120:2143–2149.
53. Horvitz HR. Nobel lecture. Worms, life and death. Biosci Rep. 2003;23:239–303.
54. Conradt B, Horvitz HR. The *elegans* protein EGL-1 is required for programmed cell death and interacts with the Bcl-2-like protein CED-9. Cell. 1998;93:519–529.
55. Yuan J, Shaham S, Ledoux S, Ellis HM, Horvitz HR. The *elegans* cell death gene *ced-3* encodes a protein similar to mammalian interleukin-1 beta-converting enzyme. Cell. 1993;75:641–652.

Figures

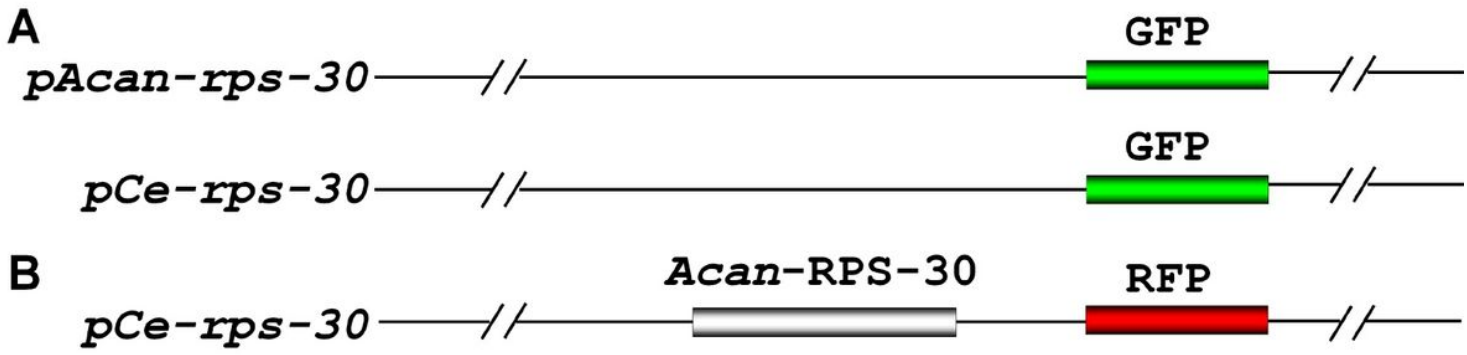

Figure 1

Cloning strategy for reporter and rescuing constructs. (A) About 2000 bp sequence upstream of Acan-rps-30 5'-UTRs was used as putative promoters. The promoter regions of Acan-rps-30 and Ce-rps-30, fused with green fluorescent protein (GFP) downstream were cloned into plasmid pPD95.77 to construct pAcan-rps-30::gfp and pCe-rps30::gfp, respectively (B) Acan-rps-30 cDNA sequence, fused with red fluorescent protein (RFP) downstream was cloned into plasmid pPD95.77, using pCe-rps30 as promoter, to construct pCe-rps-30::Acan-rps-30::rfp.

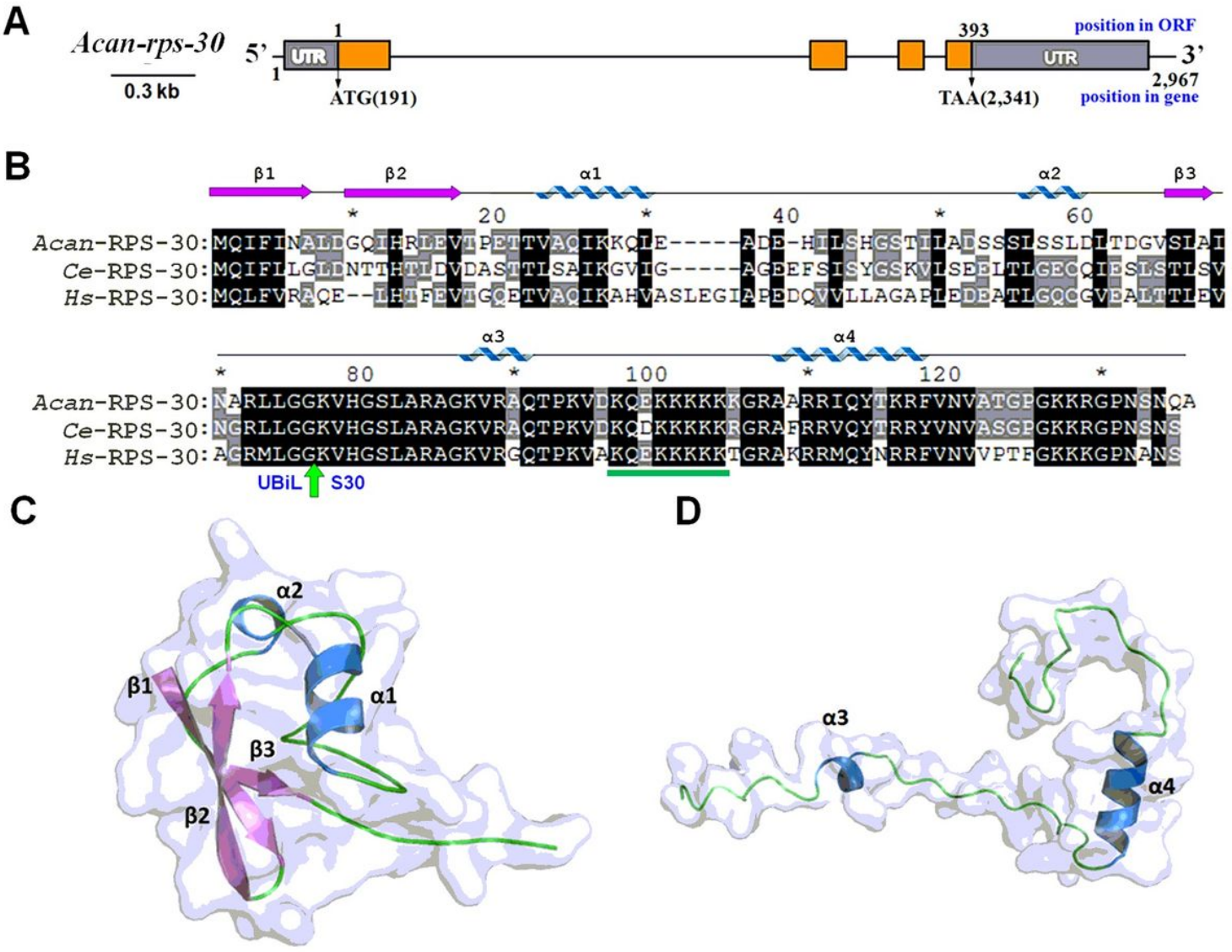

Figure 2

Structure and sequence analysis of Acan-RPS-S30. (A) The exon-intron organization of Acan-rps-30 from A. cantonensis. The Acan-rps-30 gene spans 2,967 bp, consisting of 4 exons and 3 introns. Narrow bar represented untranscribed sequences or introns; wide bars represented exons; brown blocks, coding regions; grey blocks, non-coding 5'- and 3'- untranslated region (UTR). (B) Alignment of amino acid sequences of Acan-RPS-S30 from A. cantonensis with those from Homo sapiens and Caenorhabditis elegans. The accession numbers of sequences available from current databases are: NP_505007.1 (Ce-RPS-S30) and NP_001988.1 (Hs-RPS-30). Identical and similar residues are shown in black and grey blocks, respectively. The potential cleavage sites (Gly-Gly) of the fusion protein (ubiquitin-like; UBiL-ribosome protein S30; S30) are indicated with green arrows (upstream and downstream sequences are UBiL and S30 regions, respectively). The nuclear location signals in the S30 regions are indicated with a green block. The secondary structural elements of Acan-RPS-S30 are shown above the alignment. (C) Predicted tertiary structure of UBiL region, showing 3 β-sheets and 2 α-helixes. (D) Predicted tertiary structure of S30 region, showing 2 α-helixes.

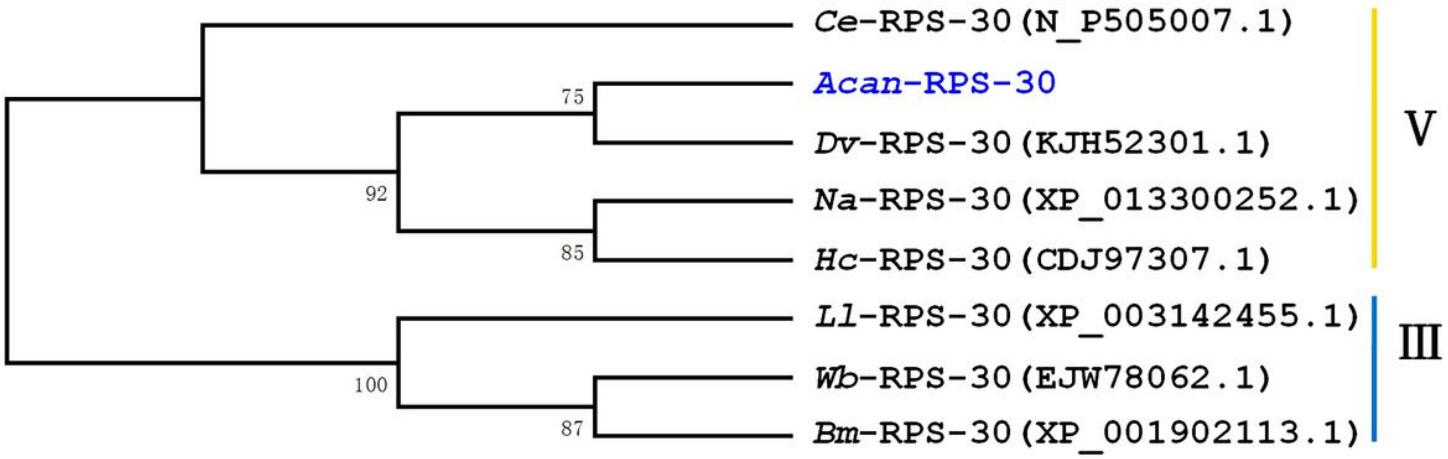

Figure 3

Neighbour-joining phylogenetic tree of RPS-30 proteins from several nematodes. The tree is calculated using the Jones–Taylor–Thornton model in the MEGA program version 5.0. Bootstrap values above the branches (1000 iterations) are shown for robust clades (> 70%). Abbreviation for species names are as follows: Ce: Caenorhabditis elegans; Acan: A. cantonensis; Dv: Dictyocaulus viviparous; Na: Necator americanus; Hc: Haemonchus contortus; Ll: Loa loa; Wb: Wuchereria bancrofti; Bm: Brugia malayi. The corresponding accession numbers are listed on the right of each species. Clade numbers were noted in Roman numerals.

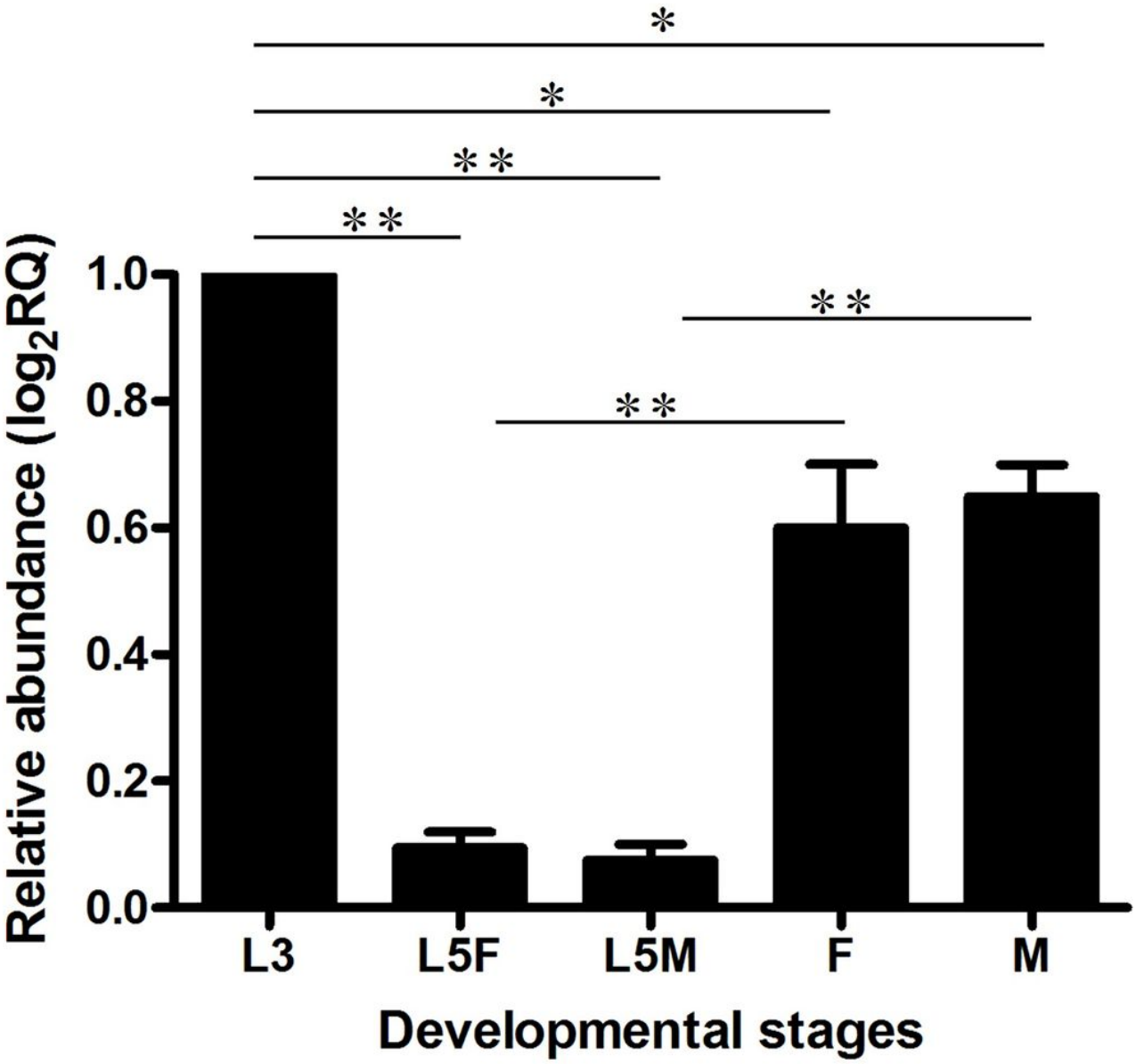

Figure 4

Transcriptional profile of Acan-rps-30 in different developmental stages (L3, L5 and adult) and genders [females (F) and males (M)] of A. cantonensis, determined by real-time PCR analysis. Data shown are mean ± S.E.M derived from three technical replicates with two biological replicates. Relative transcription of the Acan-rps-30 gene in each sample was calculated by normalisation of the raw data, followed by the determination of abundance relative to the 18S ribosomal RNA gene (GenBank: AY295804), which was served as an internal loading control. Statistical analysis was conducted using a one-way ANOVA. *P <0.05; **P<0.01.

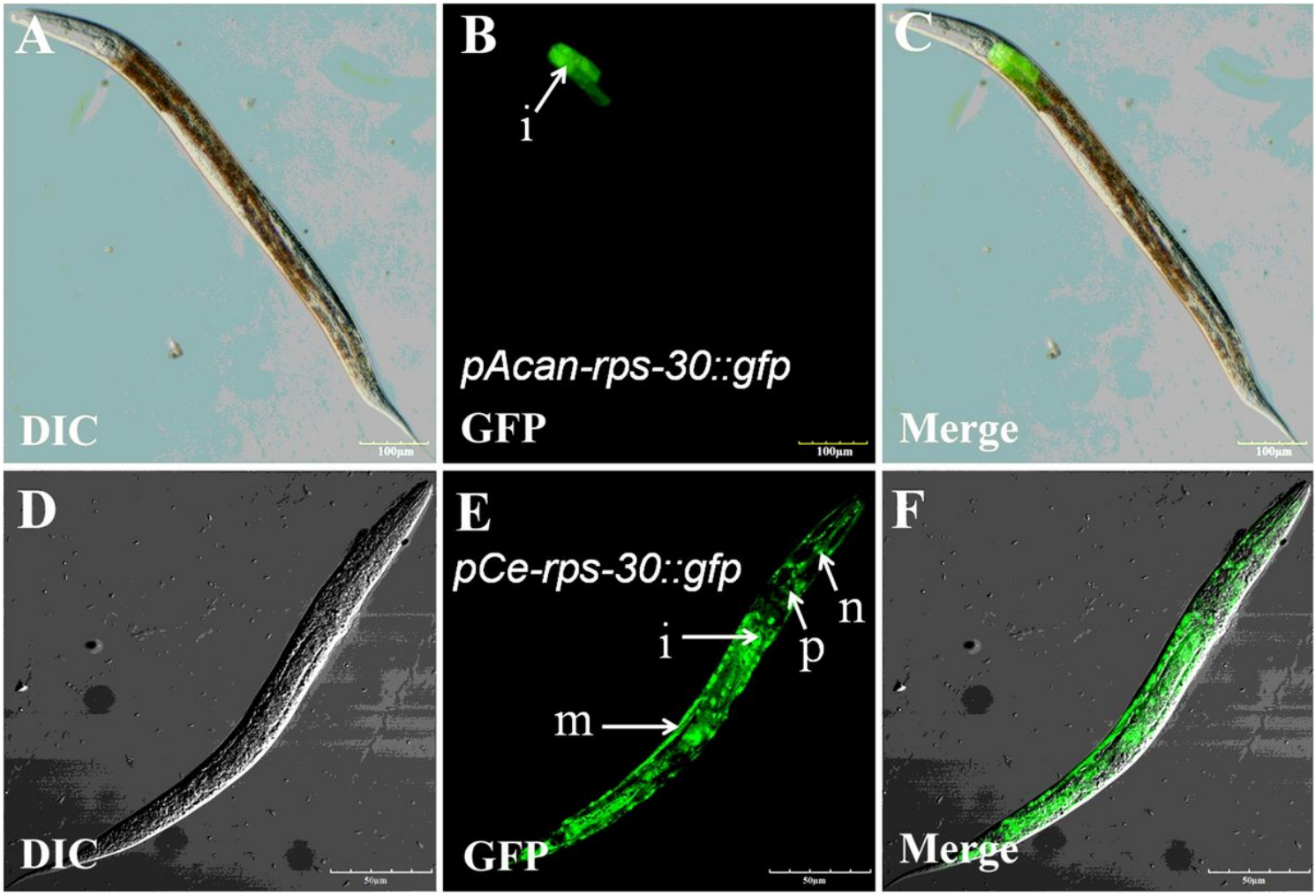

Figure 5

Expression pattern of A. cantonensis Acan-rps-30 promoter in Caenorhabditis elegans. (A-C) The promoter activity of Acan-rps-30 in C. elegans. pAcan-rps-30::gfp is only expressed in intestine, mainly in the anterior end. (D-F) The promoter activity of Ce-rps-30. pCe-rps-30::gfp is expressed ubiquitously. Arrows indicate the following tissues: i, intestinal; m, muscle; n, neuron; p, pharynx.

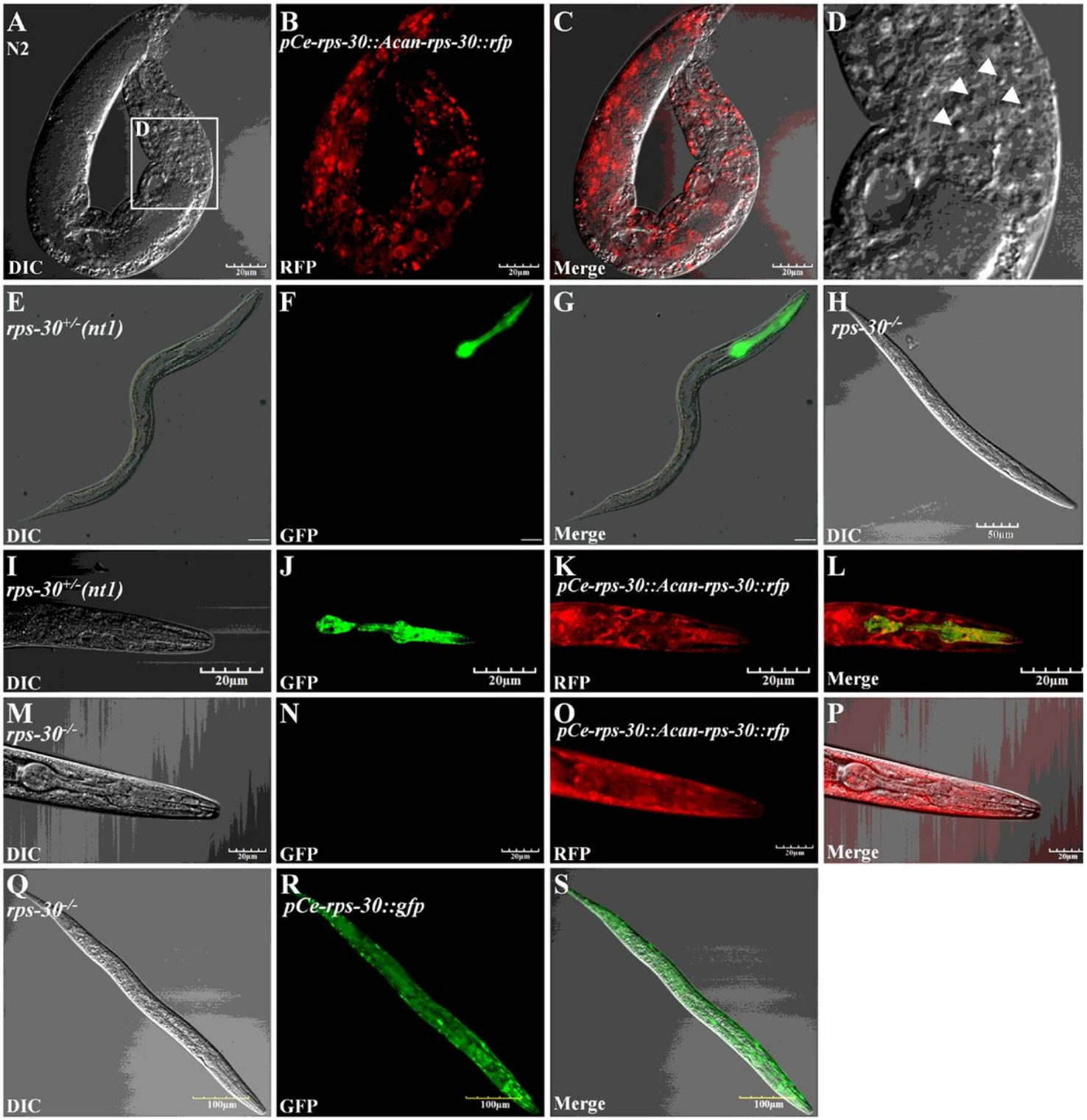

Figure 6

Cross-species expressions of Acan-RPS-30 in N2 and the rps-30 deletion mutant worms. (A-D) Expression of pCe-rps-30::Acan-rps-30::rfp in N2. RFP was expressed widely; RFP mainly focused on the nucleus; the “button-like” corpses were seen in the anterior pharynx. Arrow heads indicate the corpses. (E-G) The heterozygous rps-30+/- worm. The GFP fluorescence positive worms (pharynx) carried the balancer nT1. (H) The homozygous rps-30- /- worm. Worms without GFP (nT1) were mutation homozygous rps-30- /-. (I-

L) Expression of pCe-rps-30::Acan-rps-30::rfp in the heterozygous rps-30+/- worm. RFP was expressed widely, and GFP fluorescence was positive in pharynx. (M-P) Expression of pCe-rps-30::Acan-rps-30::rfp in the homozygous rps-30- /- worm. RFP was expressed widely, and GFP fluorescence was negative in pharynx. (Q-S) Expression of pCe-rps-30::gfp in the homozygous rps-30- /- worm.

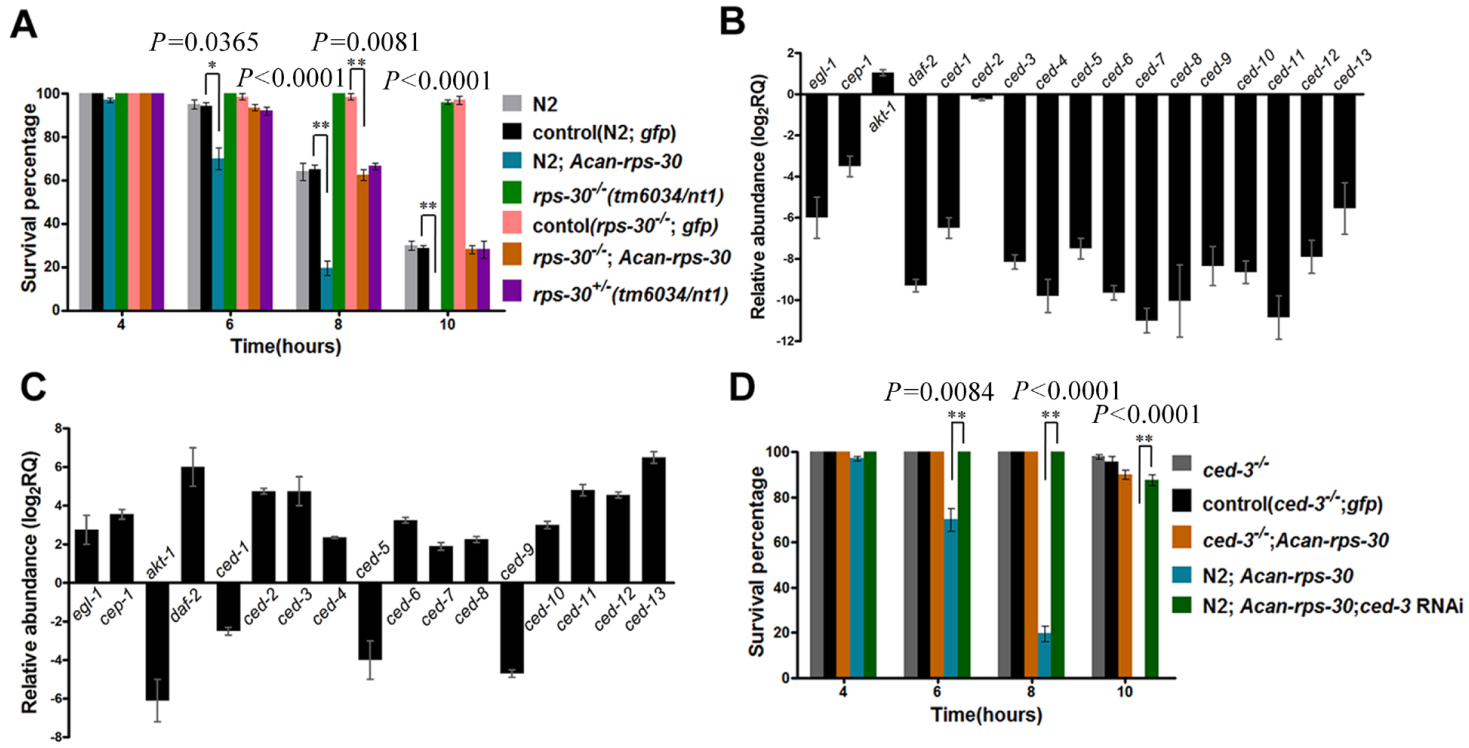

Figure 7

Down-regulated RPS-30 plays a defensive role against oxidative stress by regulating ced-3. (A) Oxidative stress assays using H2O2 in N2 and rps-30 mutant worms expressing pCe-rps30::Acan-rps-30::rfp. (B) The expression level of apoptosis genes in homozygous rps-30- /- worm. (C) The expression level of apoptosis genes in N2 worms expressing pCe-rps30::Acan-rps-30::rfp. (D) Oxidative stress assays using H2O2 in ced-3 mutant worms and worms expressing pCe-rps30::Acan-rps-30::rfp. The worms were counted as described in the “Methods” section. The error bars indicate standard deviation. *P<0.05; **P<0.01.

Supplementary Files

This is a list of supplementary files associated with this preprint. Click to download.

- TableS1.doc